horticulturae

MDPI

Article

Analysis of Floral Scent Component of Three Iris Species at Different Stages

Keyu Cai [1,†], Zhengjie Ban [1,†], Haowen Xu [2], Wanlin Chen [1], Wenxu Jia [3], Ying Zhu [4] and Hongwu Chen [1,*]

[1] College of Horticulture, Northwest A&F University, Xianyang 712100, China; caikeyu@nwafu.edu.cn (K.C.); banzhengjie@nwafu.edu.cn (Z.B.); cwl@nwafu.edu.cn (W.C.)
[2] College of Forestry, Northwest A&F University, Xianyang 712100, China; xhw@nwafu.edu.cn
[3] College of Information Engineering, Northwest A&F University, Xianyang 712100, China; jiawenxu@nwafu.edu.cn
[4] Beijing Botanical Garden Management Office, Beijing 100093, China; zhuying@chnbg.cn
* Correspondence: ylchhw1971@nwafu.edu.cn
† These authors contributed equally to this study.

Abstract: The research investigates the variations in floral scent composition among different species and developmental stages of Iris plants: *Iris uniflora*, *Iris typhifolia*, and *Iris sanguinea*. The study analyzes the fragrance components by utilizing electronic nose technology in tandem with headspace solid-phase microextraction-gas chromatography-mass spectrometry (HS-SPME-GC-MS). Principal component analysis (PCA), linear discriminant analysis (LDA), and loading analysis are applied to discern whether floral scents of the same Iris species at distinct stages could be differentiated. The results show that the electronic nose significantly distinguishes the aromas from different stages and that there are differences in aroma composition. Gas Chromatography-Mass Spectrometry confirms significant differences in volatile components regarding the three Iris species, with common compounds like alcohols, aromatics, and aldehydes present throughout stages. Notably, nonyl aldehyde, capric aldehyde, 2,4-di-tert-butylphenol, and n-heptadecane are consistently found. Cluster analysis reveals a grouping of decay stage samples of *Iris typhifolia* and *Iris sanguinea* due to terpene and ester abundance. Nonyl aldehyde significantly contributes to the aroma profiles of all species, owing to its high odor activity value. The significant content of volatile compounds in these Iris varieties suggests economic and medicinal potential beyond ornamental value, providing references for the development of Iris-scented products, aromatherapy, and the extraction of pharmacologically active substances from Iris.

Keywords: Iris; floral fragrance; GC-MS; OAV

check for updates

Citation: Cai, K.; Ban, Z.; Xu, H.; Chen, W.; Jia, W.; Zhu, Y.; Chen, H. Analysis of Floral Scent Component of Three Iris Species at Different Stages. *Horticulturae* **2024**, *10*, 153. https://doi.org/10.3390/horticulturae10020153

Academic Editor: Jiri Gruz

Received: 9 January 2024
Revised: 24 January 2024
Accepted: 5 February 2024
Published: 6 February 2024

Copyright: © 2024 by the authors. Licensee MDPI, Basel, Switzerland. This article is an open access article distributed under the terms and conditions of the Creative Commons Attribution (CC BY) license (https://creativecommons.org/licenses/by/4.0/).

1. Introduction

Floral fragrances are mainly composed of small-molecule volatile compounds, which can be extracted, collected, or biosynthesized, and are widely used in various fields, such as daily chemicals, medicine, food, and others [1]. Floral fragrances are crucial characteristics of plants, having several important functions. Plants release volatile components through flower organs to attract insects for pollination and fruit development. Additionally, floral fragrances aid in the defense of plants by attracting natural enemies and deterring potential damage. Moreover, floral fragrances enhance the ornamental value of plants. As people's understanding continues to deepen and the application of flower fragrances keeps being promoted, breeding fragrant flowers has become an important direction in flower cultivation.

To date, more than 1700 natural aroma substances have been discovered and identified in plants. Although thousands of plant floral aroma compounds have been identified, only 12 are found in more than 50% of seed plant families, such as limonene (71%), (E)-Ocimene

(71%), Myrcene (70%), and so on [2]. Observing many studied plants, it is evident that there are usually between 20 and 60 kinds of floral fragrance substances [3].

During the entire flowering process, the flower itself regulates the synthesis and volatilization of volatile components. Different plants share similar regulatory mechanisms. Generally, in the early stage of flowering, the volatilization of floral aroma components gradually increases, reaching its peak when flowers are ready for pollination [4].

In a study on the floral fragrance of the German bearded Iris [5], 219 species in 10 categories are identified, including 42 terpenes, 19 alkanes, 11 aromatic compounds, 52 esters, 41 alcohols, 17 ketones, 21 aldehydes, 9 acids, and 4 phenols. The volatile components of different species and cultivars show significant variations.

Furthermore, it should be noted that, during the flowering process, there is a certain time lag between the peak expression of the gene encoding the floral aroma synthase and the volatilization of the corresponding floral aroma components, sometimes even lasting 1 to 2 days [6,7]. These findings also indicate that the expression of structural genes that are responsible for producing floral aroma substances ultimately affects the volatilization of floral aroma compounds.

There are approximately 260 to 300 species of Iris plants worldwide, mainly distributed in the temperate regions of the northern hemisphere [8]. However, in my country's northwest region, there are 18 species of Iris, many of which remain under-explored. Some research teams have made progress in studying seed dormancy, germination characteristics, and interspecific hybridization barriers of *Iris sativa* [9].

As a traditional folk medicine, Iris plants have a long history of medicinal use and are mainly employed to treat various diseases, such as cancer, inflammation, and bacterial and viral infections [10]. Extracts from Iris plants are also utilized in treating atherosclerosis and osteoporosis [11]. Some Iris plants' roots, stems, and leaves contain precious essence, which can be ground into powder to obtain high-quality fragrance powder.

Iris uniflora stands out for its unique sweet and fragrant rhizome extract, making it a valuable raw material for perfume [12]. The floral fragrance characteristics of *Iris typhifolia* are primarily provided by its pistil, giving rise to a distinctive fresh aroma. [13]. The stems and leaves of *Iris sanguinea* can be used to make paper, while the flowers, with their large and colorful appearance, hold high ornamental value, and their rhizomes are used medicinally.

For this study, three types of Iris flowers in the bud stage, bloom stage, and decay stage are selected. It has been observed that the aroma of each flower stage can be significantly distinguished using an electronic nose, and there are notable differences in aroma components [14]. To determine the types and contents of various floral aroma substances in different flowering stages, electronic nose measurement, and headspace solid-phase microextraction gas chromatography-mass spectrometry, are employed [15–17]. The experimental results reveal the different flowering periods of the Iris and the main floral components, as well as the pattern of fragrance release.

2. Methods and Materials

2.1. Overview of the Test Field and Test Materials

In this study, flowers at various stages (bud, bloom, and decay) from three different Iris varieties, namely, *Iris uniflora*, *Iris typhifolia*, and *Iris sanguinea*, were selected as the sample subjects. The wild species of Iris used in the experiment were collected at the Caoxinzhuang Experimental Farm of Northwest A&F University in Yangling, Shaanxi Province, China. This region experiences a temperate continental monsoon climate, with an average altitude of 530 m, an average annual temperature of 12.9 °C, four distinct seasons, and sufficient sunshine conditions. *Iris uniflora*, *Iris typhifolia*, and *Iris sanguinea* in three stages—flower bud, bloom, and decay—were chosen as samples to determine the composition of floral aroma substances.

Sampling Method: Under sunny conditions, samples were collected between 8:00 a.m. and 10:00 a.m. Experimenters wore nitrile gloves, cut the inflorescences with scissors, and placed them into pre-cooled 50 mL sterile transparent plastic centrifuge tubes using liquid nitrogen. The tubes were sealed with tin foil, the bottle caps were tightened, and they were marked before being immersed in liquid nitrogen. Samples were temporarily stored in nitrogen and moved to the refrigerator as soon as possible, where they were stored at −80 °C.

Test Equipment: The ISQ&TRACE ISQ gas chromatography-mass spectrometry (GC-MS) coupled instrument (Type: QP-2010) from Shimadzu in Kyoto, Japan, PEN3 electronic nose from Airsense in Schwerin, Germany, analytical balance, manual headspace sampler, chromatographic column Rtx-1MS (30 m × 0.25 mm × 0.25 μm, Shimadzu, Kyoto, Japan), 15 mL headspace vials, foil, centrifuge tubes, etc., were used.

Before conducting the test, the laboratory air was ensured to be clean and free of odors, with minimal human presence. Before sample injection, the air was washed until the response values of all 10 sensors reached 1, indicating that the radar chart was approximately circular. Each centrifuge tube containing Iris in each flowering stage was taken out and allowed to stand for 30 min to allow the volatile matter in the headspace of the sample to reach an equilibrium state. The electronic nose sampling needle and the air supply needle were then inserted into the headspace bottle through the tin foil simultaneously for headspace sampling and detection. Each test included gas washing, zeroing, and sample injection.

2.2. Research Methodology

2.2.1. Electronic Nose

Electronic nose measurement conditions: gas flow rate 400 mL·min^{-1}, gas washing time 60 s, zeroing time 5 s, preparation time 5 s, measurement time 120 s, taking the response value of 115~117 s for data analysis. The injection flow rate is 150 mL·min^{-1}. Clean air is used as the carrier gas during cleaning, and both the flow rates of carrier gas and sample injection are 200 mL·min^{-1}. The responses of electronic nose sensors to different types of compounds are shown in Table 1. The built-in software WinMuster (Version 1.6.2) on the PEN3 was used for data collection and analysis.

Table 1. Response characteristics of each sensor of PEN3 electronic nose.

Array Serial Number	Sensor Name	Performance Description
1	W1C	aromatic
2	W5S	broadrange
3	W3C	aromatic
4	W6S	hydrogen
5	W5C	arom-aliph
6	W1S	broad-methane
7	W1W	sulphur-organic
8	W2S	broad-alcohol
9	W2W	sulph-chlor
10	W3S	methane-aliph

2.2.2. HS-SPME-GC-MS Analysis

Headspace solid-phase microextraction-gas chromatography-mass spectrometry (HS-SPME-GC-MS, Shimadzu, Kyoto, Japan) was employed in this study. Approximately 1 g of each flowering stage sample was placed in 15 mL headspace solid-phase microextraction bottles. Subsequently, 10 μL of 2-nonanone (0.008 μL·mL^{-1}), dissolved in propylene glycol, was added to the bottom of the bottle, and the bottle cap was sealed with tin foil. We utilized the SPME extraction head from the German company Supelco, model DVB/CAR/PDMS, with a diameter of 50/30 um. After equilibrating at 45 °C for 10 min, a manual headspace sampler was inserted, and extraction was performed for 30 min. Each sample was repeated four times. The manual headspace sampler was then inserted into the

inlet of the GC-MS at 250 °C for 2.5 min to completely release the aroma components in the gas chromatography-mass spectrometer [18].

Chromatographic conditions involved using an HP-5MS capillary tube (30 m × 0.25 mm × 0.25 μm, Shimadzu, Kyoto, Japan) as the chromatographic column, adopting the splitless mode. The inlet temperature was set at 250 °C, and high-purity nitrogen (99.999%) was used as the carrier gas at a flow rate of 1.0 mL·min^{-1}. The column temperature followed a heating and cooling program: the initial temperature was 40 °C, with a holding time of 3 min. The temperature was then raised to 150 °C at a rate of 5 °C·min^{-1}, followed by a further increase at a rate of 10 °C·min^{-1} to 220 °C, where it was kept for 10 min.

Mass spectrometry conditions involved the full scan mode, electron ionization (EI) as the ionization mode, an emission current of 10 Ua, electron energy of 70 eV, ion source temperature of 220 °C, transmission source temperature of 220 °C, and a mass scanning range of 35~450 amu.

For GC-MS data identification and analysis methods:

Qualitative method: The stable peak on the ion peak diagram was identified by corresponding to the first place in the preferred ranking of multiple substances under the same retention time (RT) value, starting from the first stable peak. The selected substances were compared with the four times duplicate tests to ensure they appeared at the same RT value and ranked at the top.

2.2.3. Identification and Analysis Methods

Qualitative method: Each component obtained using GC-MS analysis is searched and compared with NIST2017 mass spectrometry and a standard information database, as well as identified and analyzed together with the related literature. By using the carbon standard method, with the same column and rising and cooling procedure as GC-MS, the mixed standard of C7-C30 normal alkane is used as the standard to calculate the linear retention index (Formula (1)) of various aroma components of *Iris uniflora*, *Iris typhifolia*, and *Iris sanguinea* samples, and the results are compared with those of NIST spectrum database. Starting from the first stable peak according to the ion peak diagram, the stable peak corresponds to the first place of a variety of substances under the same RT value, and the selected substances should appear under the same RT value in the four basic biological repeats and rank in the top three.

$$LRI = 100z + 100\,(RT - RTz)/(RT\,(z + n) - RTz) \quad (1)$$

Quantitative method: Initially, 2-nonanone was chosen as the internal standard material with a density of 0.82 g/mL. The numerical equivalent of the added volume of the internal standard substance (μL) was ten times the sample mass (g). The quantification of various aroma components in the *Iris typhifolia* sample was carried out using Formula (2), and the average value was determined after four biological replicates.

$$M_i = C_0 \times V_0 \times A_i \div (A_0 \times M) \quad (2)$$

M_i is the content of each aroma component (μg/g), C_0 is the internal standard concentration (μg/μL), V_0 is the internal standard volume (μL), A_i is the peak area of the desired aroma component, A_0 is the peak area of internal standard material, and M is the sample mass (g).

OAV value: the ratio of the mass concentration of the substance (Formula (3)) to the threshold value of the substance in water, or solvent with properties similar to water (Formula (4)), is used as a standard to evaluate the contribution of the substance to the overall aroma profile of the sample, and the standard sample for aroma reconstruction is selected from it, in which the substance with OAV $\geq$ 1 is the characteristic aroma component.

$$C_i = C_0 \times A_i \div A_0 \quad (3)$$

C_i is the mass concentration of each aroma component (μg/mL), C_0 is the internal standard concentration (μg/μL), and A_i and A_0 are the peak area and internal standard peak area of the aroma component, respectively.

$$OAV = C_i \div OT_i \quad (4)$$

OT_i is the threshold value of the aroma component in water or solvent with properties similar to water (μg/mL). If there is no numerical value for the threshold of a compound in water, then the value of the closest medium in properties to water should be selected.

3. Results

Figure 1 illustrates the radar map depicting the characteristic response of three Iris species at each stage. The ten sensors exhibit varying responses to the aromas of the three Iris species, generally distributed between 1 and 10. Across all samples, sensors W1W (sulphur-organic), W1S (broad-methane), W2W (sulph-chlor), and W5S (broadrange) consistently display significantly higher response values compared to other sensors. The difference between the response values of these four sensors is notable, indicating that the major classes of substances corresponding to these sensors have higher relative contents in the floral fragrance of Iris plants at all stages.

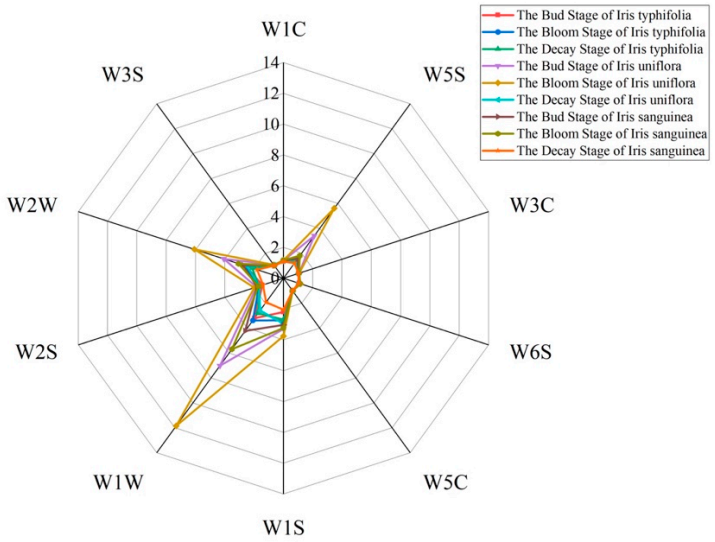

Figure 1. The radar map of the characteristic response of the volatile components in three Iris species at different stages.

During the bloom stage of *Iris uniflora*, the response values of each sensor are notably higher than those of the other eight samples. This suggests that the relative content of each type of compound in the aroma of these samples is higher compared to other stages. In the samples from various periods of *Iris typhifolia,* and the decay stage of *Iris uniflora* and *Iris sanguinea*, the response values for each sensor detecting aroma are lower, indicating a lower concentration of aromatic compounds in these samples compared to others.

In comparison with other samples, the response value of W1S replaces W5S in the top three during the decay stage of *Iris uniflora* and the decay stage of *Iris sanguinea*. This shift indicates that the relative content of methane is higher than that of nitrogen oxides in the aroma components of the samples during these three periods, while the opposite holds for other samples.

Figure 2 depicts the principal component analysis (PCA) pattern for each flowering stage of *Iris uniflora*, *Iris sanguinea*, and *Iris typhifolia*, facilitating the differentiation of floral aromas among different stages of the same Iris variety. The contribution rate of the first principal component is 97.15%, the contribution rate of the second principal component is 1.98%, and the cumulative contribution rate of the two principal components is 99.13%. This

indicates that these two principal components effectively represent the main information characteristics of the samples.

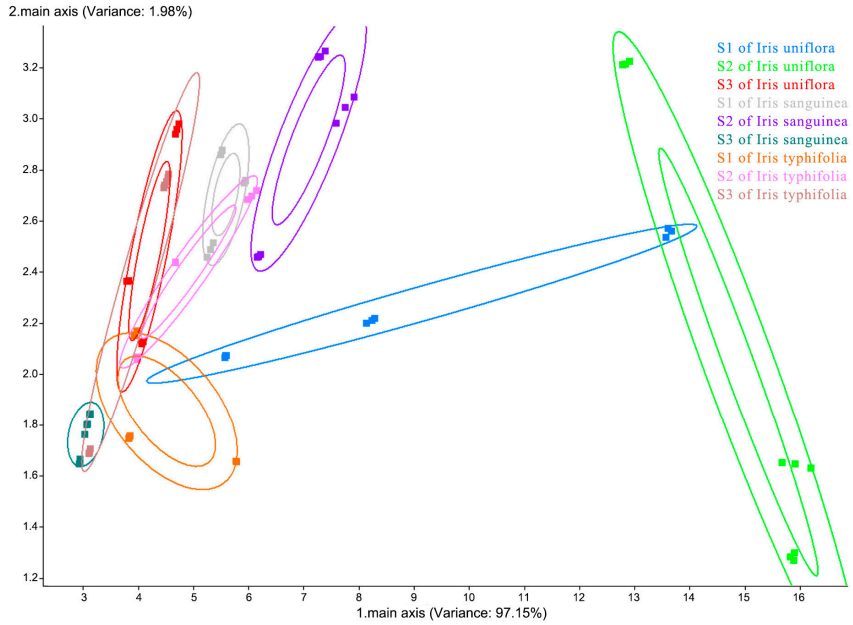

Figure 2. The PCA result of the volatile components in three Iris species at different stages. Note: S1: the bud stage, S2: the bloom stage, S3: the decay stage.

In Figure 2, it is evident that among the three types of Iris, only the bud stage, bloom stage, and decay stage of *Iris sanguinea* can be significantly distinguished. In contrast, the principal component analysis pattern diagrams for each flowering stage of *Iris uniflora* and *Iris typhifolia* exhibit overlap, indicating that they cannot be significantly differentiated in this mode. This lack of distinction is attributed to the relatively similar odors of *Iris uniflora* and *Iris typhifolia* across various periods. Principal component analysis, in this context, proves insufficient for distinguishing the internal flowering stages of *Iris uniflora* and *Iris typhifolia*.

Electronic nose loading analysis is a research method employed to distinguish volatile substances in a sample using electronic nose sensors. It primarily investigates which gas substances in the sample play a key role in this distinction and determines their contribution rates. The results of electronic nose loading analysis for each stage of *Iris uniflora*, *Iris typhifolia*, and *Iris sanguinea* are illustrated in Figure 3. The positions of sensors W1W (sulphur-organic), W2W (sulph-chlor), W1S (broad-methane), W5S (broadrange), and W2S (broad-alcohol) significantly deviate from the origin, indicating the importance of these five sensors in distinguishing the volatile components of the three Iris varieties at different stages. This observation underscores that the variations in floral composition across different periods are predominantly associated with volatile substances, such as sulphur-organic, sulph-chlor, broad-methane, broadrange, and broad-alcohol.

The results of the Linear Discriminant Analysis (LDA) for *Iris uniflora*, *Iris sanguinea*, and *Iris typhifolia* are presented in Figure 4. The contribution rate of the first discriminant factor is 76.36%, and the contribution rate of the second discriminant factor is 10.28%. The cumulative contribution rate reaches 86.64%, indicating that these two discriminant factors essentially represent the main information characteristics of the samples. Figure 4 reveals that the floral fragrances of *Iris uniflora*, *Iris sanguinea*, and *Iris typhifolia* can be significantly distinguished.

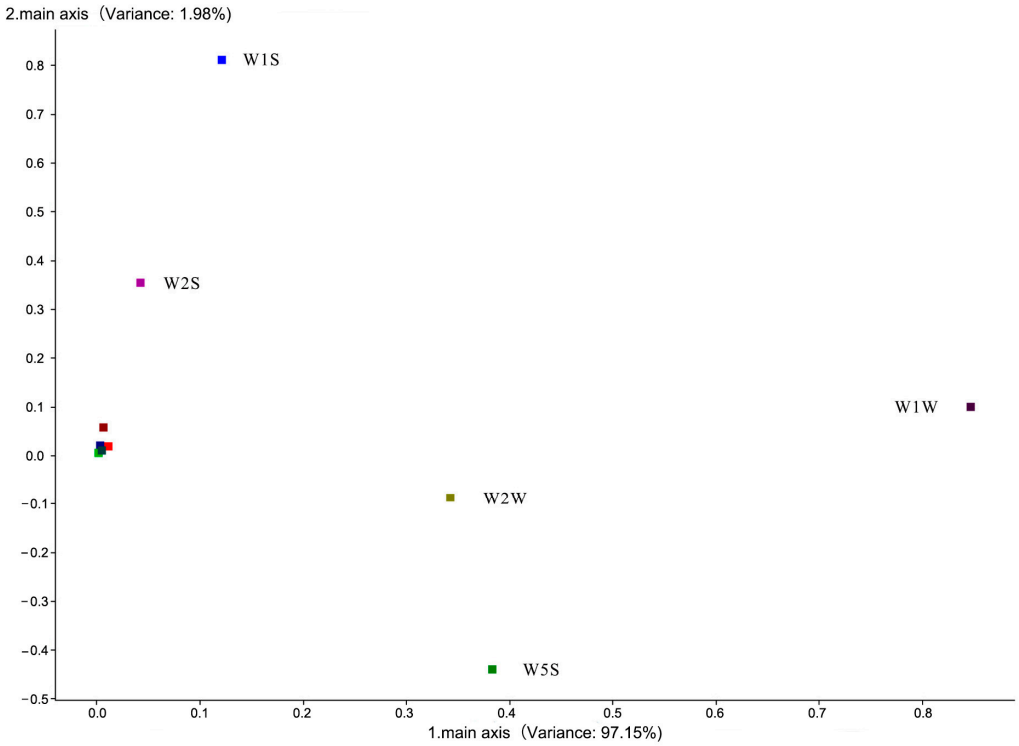

Figure 3. The loading result of the volatile components in three Iris species at different stages.

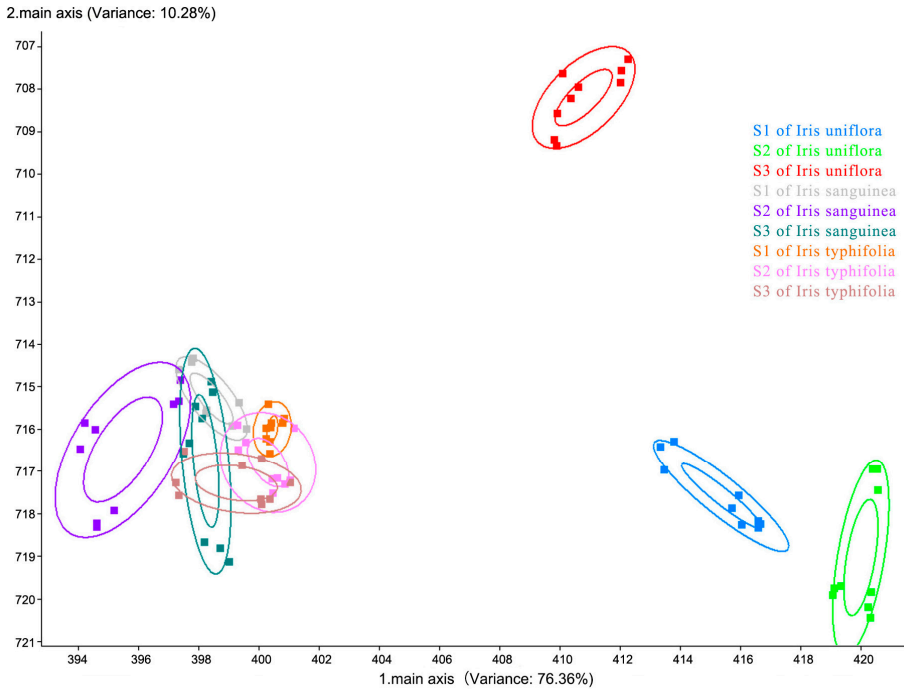

Figure 4. The LDA result of the volatile components in three Iris species at different stages. Note: S1: the bud stage, S2: the bloom stage, S3: the decay stage.

In comparison with Principal Component Analysis, Linear Discriminant Analysis demonstrates a more concentrated distribution, and its discrimination effect is notably higher than that of Principal Component Analysis.

The qualitative and quantitative determination of volatile components in *Iris typhifolia* is conducted through Gas Chromatography-Mass Spectrometry (GC-MS) and spectral library retrieval. A total of 37 species are detected in the bud stage, 43 in the bloom stage, and 39 in the decay stage. The Venn diagram in Figure 5 illustrates the floral composition across different periods, with 13 identical floral components found in all three periods, 10 unique to the bud stage, 12 in bloom, and 13 in the decay stage.

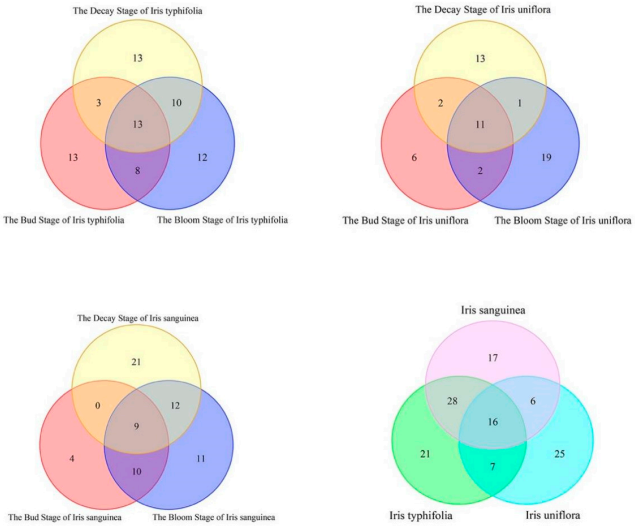

Figure 5. The Venn diagram of the numbers of volatile components in three Iris species.

Quantitative determination of volatile components in *Iris uniflora* reveals 21 species in the bud stage, 33 in the bloom stage, and 27 in the decay stage. Across the three periods, there are 11 identical floral components, 6 unique to the bud stage, 19 in bloom, and 13 in the decay stage. For *Iris sanguinea*, 23 species are detected in the bud stage, 42 in the bloom stage, and 42 in the decay stage. The three periods share 11 identical floral components, with 4 unique to the bud stage, 11 in bloom, and 21 in the decay stage.

In total, 72 species are detected in *Iris typhifolia* samples, 54 in *Iris uniflora*, and 67 in *Iris sanguinea*. The three iris species share a total of 16 identical floral components, with 21 unique to *Iris typhifolia*, 25 in *Iris uniflora*, and 17 in *Iris sanguinea*.

Figures 6 and 7 respectively depict the number and relative content of floral fragrance species in three different stages of Iris. The types of compounds present at each stage include alcohols, aromatics, aldehydes, ketones, alkanes, and esters. The relative content of aldehydes in each stage is notably high, exceeding 40% and reaching an impressive 83.23% in the flower bud stage of *Iris typhifolia*. Olefin and heterocycle samples exhibit low relative contents, less than 2%. The number of ketone species remains relatively stable across all samples over time. Terpene species are generally fewer in the bud stage but exhibit a sudden increase in the decay stage and bloom stage. Although the relative content is not high, the number of terpene species reaches 11 during the decline stage of *Iris sanguinea* and 13 during the bloom stage of *Iris typhifolia*—both having the largest number of volatile substances in each stage. However, only one species of terpene is found in *Iris uniflora* during this time, suggesting that the aroma substances in the decay stage of *Iris uniflora* do not rely on terpenes. The number of alkane species in the flower bud stage of *Iris typhifolia* is several times higher than that in the other two Iris types. In *Iris uniflora*, the number of aromaticity and alkane species gradually increases during the flower bud stage, full bloom stage, and decay stage. Alcohols are found abundantly only in *Iris uniflora*. In *Iris sanguinea*, the number of esters and ketones decreases over time, with esters having a higher quality score only in the bud stage.

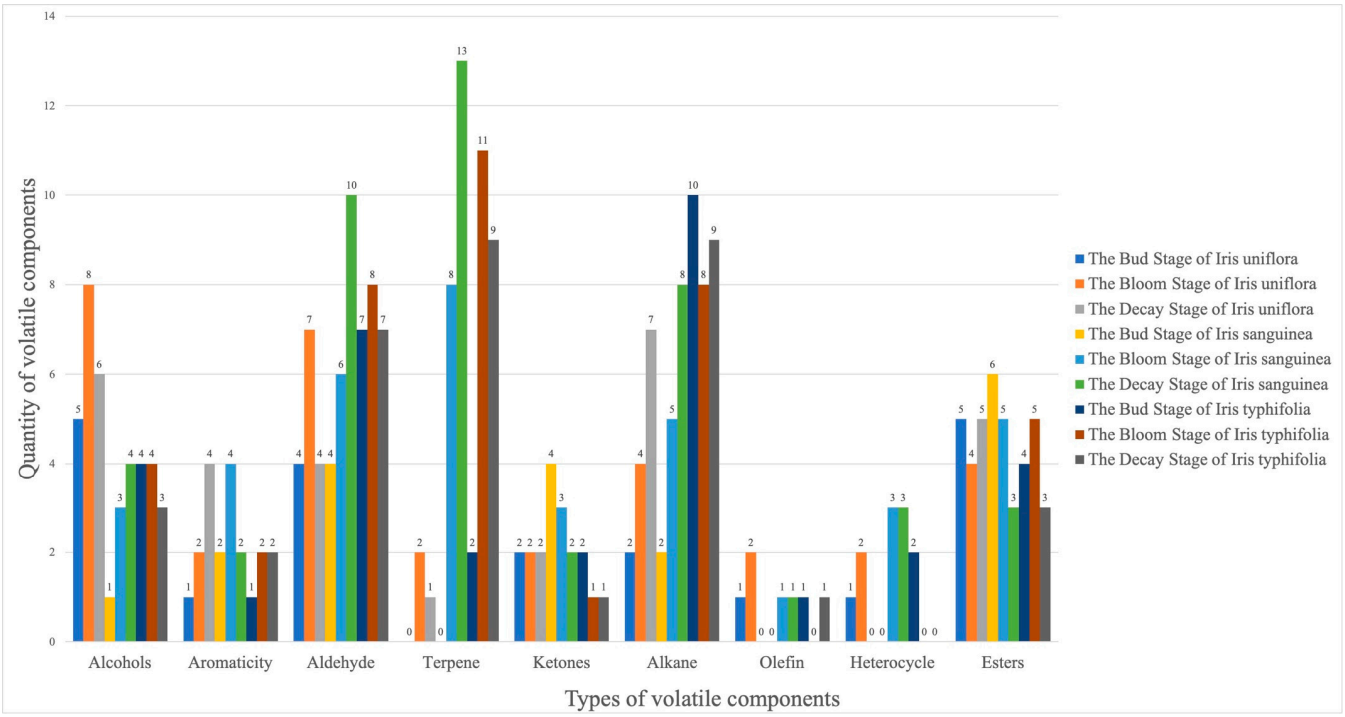

Figure 6. The number of volatile compounds in three Iris species at different stages.

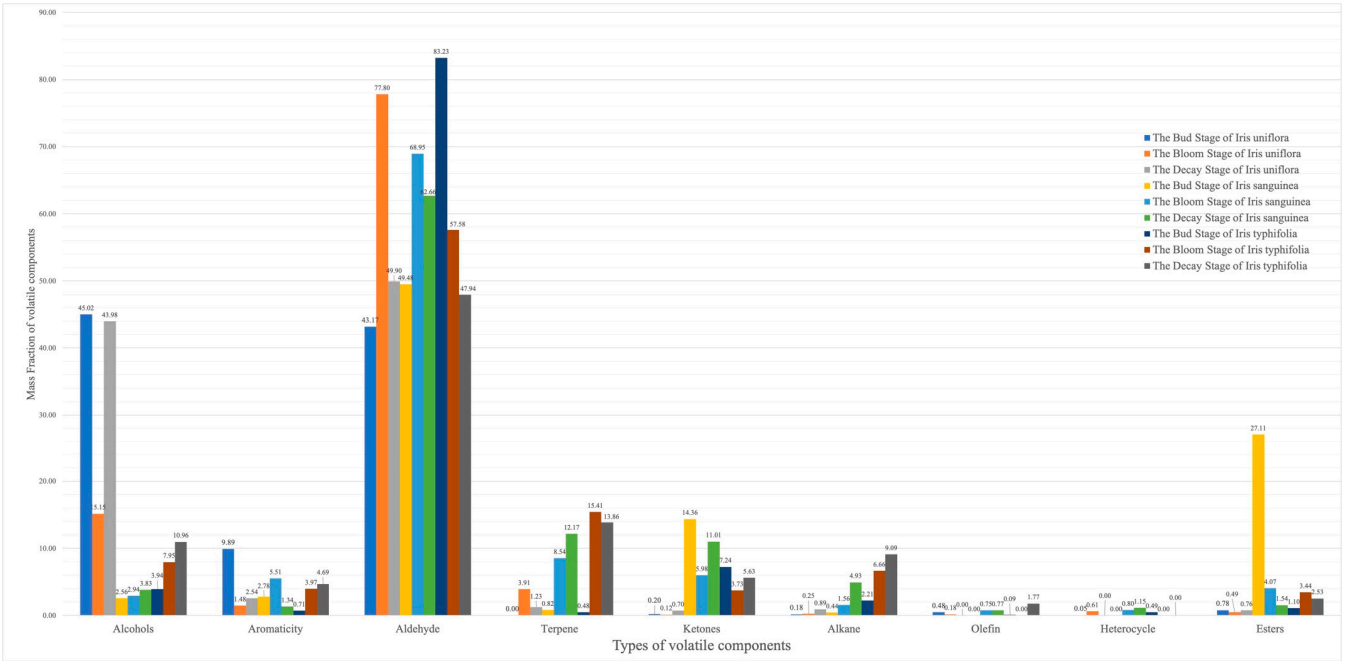

Figure 7. The relative content of volatile compounds in three Iris species at different stages.

Table 2 presents the relative content of volatile compounds from *Iris uniflora*, *Iris typhifolia*, and *Iris sanguinea* at different growth stages. Notably, nonyl aldehyde, capric aldehyde, 2,4-di-tert-butylphenol, and n-heptadecane are detected in all stages of each Iris species.

Table 2. The relative content of the compound in three Iris species at different stages (%).

Compound	Case#	The Bud Stage of *Iris uniflora*	The Bloom Stage of *Iris uniflora*	The Decay Stage of *Iris uniflora*	The Bud Stage of *Iris typhifolia*	The Bloom Stage of *Iris typhifolia*	The Decay Stage of *Iris typhifolia*	The Bud Stage of *Iris sanguinea*	The Bloom Stage of *Iris sanguinea*	The Decay Stage of *Iris sanguinea*
acetal diethyl alcohol	105-57-7	0.20		0.08						
2-hexyne-1-ol	764-60-3	8.28								
2-hexenal	505-57-7	39.02	22.38	7.30	27.06	21.02	9.11			6.09
3-hexenol	544-12-7	20.00	9.43	23.00				2.56	1.65	
N-hexyl alcohol	111-27-3	16.07	3.66	17.23					0.97	1.15
N-caprylic aldehyde	124-13-0	0.83	0.39							
Eudinol	470-82-6	0.47								
3,7-dimethyl-1,3,7-octtriene	502-99-8	0.48								
2-isopropyl-3-methoxypyrazine	25773-40-4	0.05								
nonyl aldehyde	124-19-6	2.36	1.70	1.33	1.56	2.14	8.29	1.16	0.44	3.95
capric aldehyde	112-31-2	0.95	0.42	0.16	0.10	0.65	6.83	0.75	0.24	1.31
methyl caprate	110-42-9	0.22	0.06		0.53	0.40		9.68	1.46	
ethyl caprate	110-38-3	0.22	0.32	0.58	0.14	0.96		11.60	1.54	
geranyl acetone	3796-70-1	0.14						0.34		
2,4-di-tert-butylphenol	96-76-4	9.89	1.43	1.92	0.71	3.41	1.42	2.33	1.03	0.70
2,2,4-trimethyl-1,3-pentanediol diisobutyrate	6846-50-0	0.11						0.28		
n-cetane	544-76-3	0.09	0.05	0.09	0.25	1.04	0.96			0.21
n-heptadecane	629-78-7	0.09	0.10	0.05	0.16	0.72	1.01	0.14	0.17	0.40
diisobutyl phthalate	84-69-5	0.07					0.30			0.18
7,9-di-tert-butyl-1-oxacanthin[4,5]decan-6,9-diene-2,8-dione	82304-66-3	0.05		0.03						
Dibutyl phthalate	84-74-2	0.16	0.07	0.07				0.27	0.12	
3-methyl-3-butenol	763-32-6		0.30							
Cis-2-pentenol	1576-95-0		0.42			0.61				
2-methyl-4-valeraldehyde	5187-71-3		52.68		27.06					
(1-methylamyl) cyclopropane	6976-28-9		0.06							
enanthal	111-71-7		0.21		0.29	0.26	1.56			0.98

Table 2. *Cont.*

Compound	Case#	The Bud Stage of *Iris uniflora*	The Bloom Stage of *Iris uniflora*	The Decay Stage of *Iris uniflora*	The Bud Stage of *Iris typhifolia*	The Bloom Stage of *Iris typhifolia*	The Decay Stage of *Iris typhifolia*	The Bud Stage of *Iris sanguinea*	The Bloom Stage of *Iris sanguinea*	The Decay Stage of *Iris sanguinea*
2-ethylfuran	3208-16-0		0.57		0.28				0.54	0.25
α-pinene	80-56-8		0.36		0.19		1.76		2.26	1.50
ocimene	13877-91-3		3.55	1.23		2.07				0.35
cis-α,α-5-trimethyl-5-vinyltetrahydrofuran-2-methanol	5989-33-3		0.13							
linalool	78-70-6		1.05		0.25	6.10	4.06		0.32	0.23
2,6-dimethyl-2,4,6-octtriene	3016-19-1		0.07							
2-methoxy-3-sec-butylpyrazine	24168-70-5		0.04		0.20				0.15	0.41
undecanal	112-44-7		0.02		0.12					0.30
ionone	127-41-3		0.06							
β-zirodone	79-77-6		0.07							
2,6,11-trimethyldodecane	31295-56-4		0.04		0.24		1.14			
trans-neroli tertiary alcohol	40716-66-3		0.09							
4-sec-butyl-2,6-di-tert-butylphenol	17540-75-9		0.05							
6,9-heptadecadiene	81265-03-4		0.11							
3-hexenal	4440-65-7			41.10		21.47				
trans-3-hexenol	928-97-2			0.75						2.12
trans-2-hexene-1-ol	928-95-0			0.94						
3-ethyltoluene	620-14-4			0.13						
mesitylene	108-67-8			0.30						
4-ethyltoluene	622-96-8			0.20						
decane	124-18-5			0.24						
2,6-dimethyl-nonane	17302-28-2			0.18						
n-dodecane	112-40-3			0.22	0.28	0.31	0.72		0.14	
undecane	1120-21-4			0.11						
transnon-2-enol	31502-14-4			1.99						

Table 2. *Cont.*

Compound	Case#	The Bud Stage of *Iris uniflora*	The Bloom Stage of *Iris uniflora*	The Decay Stage of *Iris uniflora*	The Bud Stage of *Iris typhifolia*	The Bloom Stage of *Iris typhifolia*	The Decay Stage of *Iris typhifolia*	The Bud Stage of *Iris sanguinea*	The Bloom Stage of *Iris sanguinea*	The Decay Stage of *Iris sanguinea*
2,2,4-trimethyl-1,3-pentanediol monoisobutyrate	25265-77-4			0.07						
2,2,4-trimethylpentanediol isobutyl ester	6846-50-0			0.04						
phytoketone	502-69-2			0.67						
pentene-3-ol	616-25-1				0.46	0.91				
1-pentene-3-ketone	1629-58-9				0.68			0.68	0.37	
cis-2-pentenol	1576-95-0				0.35					
trans-2-hexenal	6728-26-3				27.06				2.20	
leaf alcohol	928-96-1				2.88		6.32			
6-methylhept-5-en-2-one	110-93-0				6.56		5.63			7.57
basil isomer mixture	13877-91-3				0.29					
methyl caprylate	111-11-5				0.13			2.26	0.55	
tridecane	629-50-5				0.21					
1-tetradecene	1120-36-1				0.09					
tetradecane	629-59-4				0.31	0.62	1.03		0.09	0.38
n-nonadecane	629-92-5				0.11		0.58			
2,6,10-trimethyldodecane	3891-98-3				0.27					
n-pentadecane	629-62-9				0.27	0.85		0.31	0.23	
n-octadecane	593-45-3				0.12	0.59				0.35
diethylhexyl carbonate	14858-73-2				0.30					
1,2-dichloroethane	107-06-2					1.90				
chlorophyllin aldehyde	6728-26-3					10.60		6.35		
2-pinene	2437-95-8					5.05				
β-pinene	18172-67-3					0.77				
methyl heptenone	110-93-0					3.73		12.88	5.18	
D-terpenediene	5989-27-5					4.87				
(E)-B-basil	3779-61-1					0.24				

Table 2. *Cont.*

Compound	Case#	The Bud Stage of *Iris uniflora*	The Bloom Stage of *Iris uniflora*	The Decay Stage of *Iris uniflora*	The Bud Stage of *Iris typhifolia*	The Bloom Stage of *Iris typhifolia*	The Decay Stage of *Iris typhifolia*	The Bud Stage of *Iris sanguinea*	The Bloom Stage of *Iris sanguinea*	The Decay Stage of *Iris sanguinea*
phenylacetaldehyde	122-78-1					1.13	1.59		0.30	0.52
octyl formate	112-32-3					0.40				
phenylacetonitrile	140-29-4					0.32			0.13	
1-nonyl alcohol	143-08-8					0.32				
methyl salicylate	119-36-8		0.03			1.26	1.34			0.69
B-Nitrophenethane	6125-24-2					0.57			4.21	
n-tridecane	629-50-5					0.63				
alcohol ester-12	77-68-9					0.41				
alpha-pinene	3856-25-5					0.90	1.05			0.77
1-caryophyllene	87-44-5					0.36				
A-bergamonene	17699-05-7					0.50				0.46
α-caryophyllene	6753-98-6					0.25				
A-curcumene	644-30-4					0.23				
γ-juniperene	39029-41-9					0.19				
isovaleric aldehyde	590-86-3						0.60			0.33
n-caproaldehyde	66-25-1						19.97	41.22	65.62	45.94
(E,E)-2,4-hexadienal	142-83-6						1.77			
1-octen-3-ol	3391-86-4						0.57			0.33
terpinene	99-86-5						1.82			0.54
O-isopropyl benzene	527-84-4						3.27			0.64
γ-terpinene	99-85-4						1.82			
4-terpenol	562-74-3						2.84			0.67
2,7,10-trimethyldodecane	74645-98-0						1.05			
2-methyl-propionate 3-hydroxy-2,2,4-trimethyl-amyl ester	77-68-9						0.88			0.66
B-bourbon	5208-59-3						1.32			0.81
β-caryophyllene	87-44-5						1.53		0.10	1.49

Table 2. *Cont.*

Compound	Case#	The Bud Stage of *Iris uniflora*	The Bloom Stage of *Iris uniflora*	The Decay Stage of *Iris uniflora*	The Bud Stage of *Iris typhifolia*	The Bloom Stage of *Iris typhifolia*	The Decay Stage of *Iris typhifolia*	The Bud Stage of *Iris sanguinea*	The Bloom Stage of *Iris sanguinea*	The Decay Stage of *Iris sanguinea*
alpha-trachene	6753-98-6						1.00			0.90
Γ-juniperene	39029-41-9						0.74			0.54
2,6,10,15-tetramethylheptadecane	54833-48-6						1.12			0.50
N-heptacosane	593-49-7						1.48			
p-xylene	106-42-3							0.45		
acetophenone	98-86-2							0.47	0.44	3.44
ethyl caprylate	106-32-1							3.02	0.40	
N-decanoic acid	334-48-5							0.82		
3-methyl-2-butenal	107-86-8								0.14	
3-ethylthiophene	1795-01-3								0.11	
α-cresine	99-83-2								0.06	
L-beta-pinene	18172-67-3								0.43	
4-isopropyl toluene	99-87-6								0.14	
(+)-limonene	5989-27-5								5.09	1.60
3,6,6-trimethyl-bicyclic(3,1,1)hept-2-ene	4889-83-2								0.13	
(Z)-3,7-dimethyl-1,3,6-octadecatriene	3338-55-4								0.92	
allobasil	7216-56-0								0.19	
(-)-alpha-pinene	3856-25-5								0.34	
trans-squalene	111-02-4								0.06	
n-valeraldehyde	110-62-3									0.33
2-methylheptane	592-27-8									0.61
2,4-dimethylheptane	2213-23-2									2.20
narcocapsicum tomakomai	20697-20-5									0.49
dodecane	112-40-3									0.29
(-)-α-cubebeene	17699-14-8									0.77
e-β-farnesene	18794-84-8									0.93
Δ-juniperene	483-76-1									1.60

For *Iris uniflora*, 2-hexenal, 3-hexenol, and n-hexyl alcohol are consistently detected across growth stages, with relative contents exceeding 1%. Additionally, 2-methyl-4-valeraldehyde is present with a relative content of 52.68% during the bloom stage but remains undetectable during the bud and decay stages. The relative content of 3-hexenal is 41.10% during the decay stage but is not detected during the bud and bloom stages.

In *Iris typhifolia*, only nonyl aldehyde is consistently detected throughout all growth stages with relative contents exceeding 1%. 2-hexenal is abundant during the bud and bloom stages but remains undetectable during the decay stage. Both (1-methylamyl) cyclopropane and trans-2-hexenal are present in significant amounts during the bud stage but cannot be detected during the other stages.

For *Iris sanguinea*, nonyl aldehyde, capric aldehyde, n-heptadecane, 2,4-di-tert-butylphenol, and n-caproaldehyde are detected across all stages, with n-caproaldehyde consistently having relative contents above 40% throughout the stages.

The cluster analysis heatmap for the three stages of three Iris species is depicted in Figure 8, where color blocks transition from blue to red, indicating a decreasing trend in quality scores.

The nine sample groups can be classified into two major clusters. In the primary classification, the decay stage of *Iris typhifolia* and the decay stage of *Iris sanguinea* are grouped together due to their similarities in volatile terpenoids and esters, resulting in relatively high-quality scores. These two stages also exhibit distinct differences from the other samples, forming a separate cluster along with the remaining seven samples. The heatmap illustrates significant variations in both the types and concentrations of volatile substances among the nine sample groups. The clustering analysis results align with the aroma discrimination obtained from the electronic nose, indicating distinct aromatic profiles among the three Iris species at different stages.

The volatile substances in different groups show noticeable differences and can be categorized into four clusters. Cluster 1 primarily consists of terpenoid compounds, with higher concentrations observed in the bloom stage of *Iris sanguinea* and the decay stage of *Iris sanguinea* samples. Cluster 2 shows higher levels in the decay stage of *Iris typhifolia* and moderate levels in the decay stage of *Iris sanguinea*. Cluster 3 exhibits relatively higher concentrations in the bud stage of *Iris uniflora*.

The Odor Activity Value (OAV) serves as the primary criterion for determining the overall contribution of volatile compounds to a sample's aroma. Based on previously reported aroma threshold values, OAV values for three Iris species have been calculated in Table 3. This criterion is used to assess the contribution of each substance to the overall aroma profile of the sample, providing a reference for selecting aroma reconstitution standard samples in subsequent experiments.

In total, 20 compounds are found to have OAV values greater than 1 in at least one stage of Iris, including 9 aldehydes, 4 terpenes, 3 alcohols, 2 esters, 1 ketone, and 1 aromatic compound. These compounds significantly contribute to the aroma profile of the sample.

Nonyl aldehyde exhibits significantly high OAV at all stages of three Iris species, imparting distinctive oily and sweet orange aromas to the flowers. Among *Iris typhifolia*, capric aldehyde demonstrates elevated OAVs during all three stages, contributing a citrusy fragrance to the blossoms. During the bud stage, n-caprylic aldehyde displays a higher OAV, providing a fruity scent. 2-hexenal registers elevated OAV during the bloom and decay stages, giving a green leafy aroma to the flowers. The linalool attains higher OAV during the bloom and decay stages of *Iris typhifolia*. Moreover, the grassy note of n-caproaldehyde plays a contributory role in shaping the olfactory profile of Iris species during the decay stage of *Iris typhifolia*, as well as the bud and bloom stages of *Iris sanguinea*.

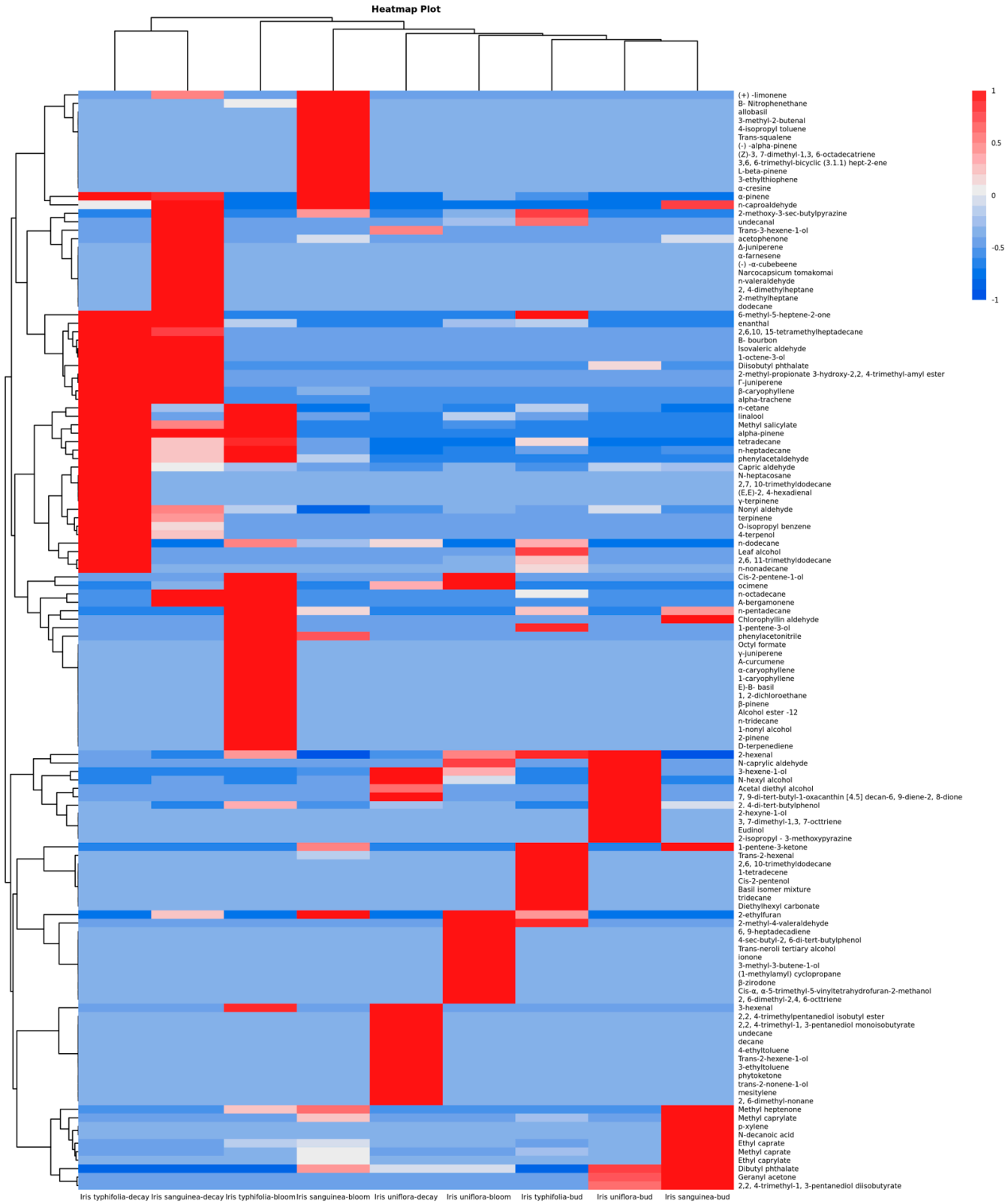

Figure 8. The cluster analysis heatmap plot of volatile compounds in three Iris species at different stages.

Table 3. The OAV of volatile compounds in three Iris species at different stages.

Compound	Threshold (μg/kg)	The Bud Stage of *Iris uniflora*	The Bloom Stage of *Iris uniflora*	The Decay Stage of *Iris uniflora*	The Bud Stage of *Iris typhifolia*	The Bloom Stage of *Iris typhifolia*	The Decay Stage of *Iris typhifolia*	The Bud Stage of *Iris sanguinea*	The Bloom Stage of *Iris sanguinea*	The Decay Stage of *Iris sanguinea*
Acetal diethyl alcohol	0.1	7.78		5.28						
2-hexenal	0.15	118.30	394.26	325.83	87.62	64.47				18.57
N-hexyl alcohol	8	7.86	1.28	14.39					0.11	0.66
N-caprylic aldehyde	0.001	3266.84	126.92							
Eudinol	0.01	185.90								
Nonyl aldehyde	0.0035	2638.26	1284.40	2547.50	217.11	281.66	475.72	298.44	117.33	516.43
Capric aldehyde	0.005	745.33	223.73	218.13	9.80	6.57	274.42	135.65	44.11	119.63
Ethyl caprate	0.2	4.29	4.28	19.32	0.35	2.21		52.34	7.94	
enanthal	0.031		17.99		4.47	3.97	1.18			14.48
linalool	0.0015		185.36		8.53	1872.43	544.47		197.87	71.36
undecanal	0.014		3.42		4.43					9.84
Chlorophyllin aldehyde	0.15					32.51		38.30		
2-pinene	0.12					19.34				
Methyl heptenone	0.1					17.15		116.18	47.82	
D-terpenediene	0.22					1.18				
phenylacetaldehyde	0.009					57.53	35.58		31.76	26.63
Methyl salicylate	0.06					9.65	4.53			5.27
alpha-pinene	0.12					3.47	1.77			2.93
n-caproaldehyde	0.0075						535.11	4958.52	878.13	28.71
alpha-trachene	0.16						1.25			2.58

The values of threshold are from Compilations of flavour threshold values in water and other media (second enlarged and revised edition) written by V. Gemert.

4. Discussion

This study investigates differences in floral scent composition among various species and developmental stages of Iris plants, specifically *Iris uniflora*, *Iris typhifolia*, and *Iris sanguinea*. PCA results indicate that the cumulative contribution rates of the first two principal components for the nine samples reach 99.13%, with only the floral scents of *Iris typhifolia* at different stages significantly differentiated. However, due to their similar fragrances, the PCA pattern plots for *Iris uniflora* and *Iris typhifolia*, overlapping in various flowering periods, do not show significant differentiation. With Linear Discriminant Analysis, the cumulative contribution rate reaches 86.64%, effectively distinguishing the floral scent samples at different stages of the same species.

Sensor contribution analysis reveals that five sensors, namely W1W, W2W, W1S, W5S, and W2S, are most sensitive to identifying floral scents from the three Iris species at various stages, playing a significant role in differentiation. The results indicate substantial differences in floral fragrances, and the variations in floral scent components among different samples are mainly related to sulfur compounds, terpenes, organic sulfur compounds, aromatic compounds, methane, nitrogen compounds, and alcohols. This conclusion provides a theoretical foundation and evidence for subsequent Gas Chromatography-Mass Spectrometry (GC-MS) analysis.

The application of headspace solid-phase microextraction-gas chromatography-mass spectrometry confirms significant differences in volatile components among the three Iris species. Throughout all stages, common volatile compounds include alcohols, aromatics, aldehydes, ketones, alkanes, and esters. Among these compounds, nonyl aldehyde, capric aldehyde, 2,4-di-tert-butylphenol, and n-heptadecane are present in all samples. Cluster analysis reveals that the decay stage samples of *Iris typhifolia* and *Iris sanguinea* are grouped together due to their high levels of terpenes and esters. This grouping stems from the abundant presence of terpenes during the decay stages of these two Iris species. Nonyl aldehyde significantly contributes to the aroma profile of the three Iris species during all stages, owing to its high odor activity value (OAV).

In the case of *Iris uniflora*, the prominent presence of 2-methyl-4-glutaraldehyde indicates its utility as an intermediate in the synthesis of the medicinal compound sleepertone and an insecticide [19]. 3-hexenol, renowned for its refreshing scent, is a crucial aromatic ingredient in perfumery production worldwide [20]. Additionally, 3-hexenal, known for its strong grassy and apple-like aroma, is approved for use as a food flavoring [21]. The inclusion of α-pinene not only offers inhibition against *Candida albicans* but also serves as a raw material for soap and detergent manufacturing [22].

Many compounds with economic and medicinal value were detected in different flower samples. In the analysis of *Iris typhifolia*, notable constituents with high relative contents include 2-hexenal, which can be applied in food additives and organic synthesis intermediates [23]. Compounds such as acetaldehyde, nonanal, trans-2-hexenal, 6-methyl-5-hepten-2-one, geraniol, decanal, and heptanal are extensively employed in edible fragrance formulations [24–30]. 2,4-di-tert-butylphenol is primarily used in the production of natural rubber and synthetic rubber antioxidants, plastic stabilizers, fuel stabilizers, UV absorbers, as well as intermediates in pesticides and dye production [31]. Linalool can be harnessed for basil alcohol production and is valued for its anti-inflammatory and antimicrobial properties [32]. The application of 2-pinenes encompasses the synthesis of pine oil alcohol, linalool, and some sandalwood-scented fragrances [33]. Methyl heptenone contributes to the synthesis of ionone and citral, being of great significance as a pharmaceutical intermediate [34]. Methyl salicylate serves as a precursor for acetylsalicylic acid synthesis [35]. Moreover, n-hexanal can be utilized as a plasticizer, an organic synthetic component in rubber and resin, an insecticide, and an edible flavoring [36]. Terpinene, recognized for its antioxidant efficacy, serves as an antioxidant in cosmetics and a food additive, which predominantly is regarded as a flavoring and preservative [37]. O-isopropylbenzene is primarily employed in creating imitation products and fixed fragrances [38]. β-Caryophyllene is mainly used for preparing fine imitation products and fragrance fixatives [39].

Regarding *Iris sanguinea*, detected volatile substances include methyl octanoate, commonly used in the production of surfactants and fragrances [40]. Ethyl octanoate gives a coconut fragrance and is predominantly utilized in the formulation of edible flavorings [41]. Methyl caproate can be applied in the preparation of pineapple, berry, and fruit-scented fragrances [42]. Ethyl octanoate serves as an enhancer for fragrances, contributing to scents like orange, strawberry, and pineapple [43]. β-Nitrophenylethane holds a pivotal role as a key chemical precursor and is utilized in numerous pharmaceuticals and dye intermediates, such as aniline, dinitrobenzene, diphenylamine, azobenzene, and m-amino benzene sulfonic acid. (+)-Limonene possesses antitussive, expectorant, and antibacterial properties [44]. n-Hexanol is instrumental in the formulation of coconut and berry-flavored fragrances [45]. 2,4-dimethyl heptane is utilized as a solvent, fragrance ingredient, organic synthesis intermediate, and herbicide [46]. Δ-Junipene offers antibacterial effects, aids in stimulating digestive enzymes, and possesses diuretic properties [47].

The high contents of certain volatile compounds in three varieties of Iris indicate that they have significant economic and medicinal potentials besides their well-known ornamental value. This provides a theoretical foundation for the development of Iris-scented perfumes, extraction of fragrance compounds, and application in aromatherapy.

5. Conclusions

This study delves into the nuanced variations in floral scent composition among three Iris plant species: *Iris uniflora*, *Iris typhifolia*, and *Iris sanguinea*, spanning various developmental stages. Utilizing advanced electronic nose technology and headspace solid-phase microextraction-gas chromatography-mass spectrometry (HS-SPME-GC-MS), the research reveals substantial transformations in the aromatic profiles of Iris flowers throughout their developmental stages.

Electronic nose measurements, complemented by principal component analysis (PCA) and linear discriminant analysis (LDA), demonstrate the ability to distinguish the floral scents of *Iris typhifolia*, *Iris sanguinea*, and *Iris uniflora* at various growth stages. Sensor contribution analysis underscores the significance of specific sensors in identifying key volatile compounds, with sulfur compounds, terpenes, organic sulfur compounds, aromatics, methane, nitrogen compounds, and alcohols emerging as pivotal contributors to these differentiating scents.

Gas chromatography-mass spectrometry (GC-MS) further elucidates significant disparities in volatile components across the three Iris species, consistently detecting common compounds, such as nonyl aldehyde, capric aldehyde, 2,4-di-tert-butylphenol, and n-heptadecane throughout the developmental stages. Cluster analysis confirms distinct aromatic profiles among the Iris species, particularly highlighting the abundance of terpenoids and esters in the decay stages of *Iris typhifolia* and *Iris sanguinea*. The study underscores the economic and medicinal potential of these Iris varieties, extending their value beyond ornamental purposes. Compounds like 2-hexenal, 3-hexenol, linalool, and n-hexyl alcohol hold promise for fragrance production, while others like nonanal, geraniol, and acetaldehyde find applications in edible fragrance formulations. Methyl salicylate, limonene, B-nitrostyrene, etc., serve as crucial raw materials for pharmaceutical synthesis.

In conclusion, this research enhances our understanding of the diverse floral scents within the Iris genus, paving the way for the development of Iris-scented products and exploring their broader economic and medicinal potential. The findings contribute to the future development of Iris's medicinal value and the application of Iris-scented perfume, essential oil, and aromatherapy.

Supplementary Materials: The following supporting information can be downloaded at: https://www.mdpi.com/article/10.3390/horticulturae10020153/s1.

Author Contributions: Conceptualization, K.C., Z.B., H.X., W.C., W.J. and H.C.; Methodology, K.C., Z.B., H.X., W.C., W.J. and H.C.; Software, W.C., W.J. and H.C.; Validation, K.C., Z.B., H.X. and W.J.; Formal analysis, K.C., Z.B. and H.X.; Resources, Y.Z.; Data curation, K.C. and W.J.; Writing—original

draft, K.C., Z.B., H.X., W.C. and W.J.; Writing—review & editing, K.C., Y.Z. and H.C; Visualization, W.J.; Supervision, Y.Z. and H.C.; Project administration, H.C.; Funding acquisition, Y.Z. and H.C. All authors have read and agreed to the published version of the manuscript.

Funding: This work was financially supported by the National Natural Science Foundation of China (31701962) and the Beijing Municipal Park Management Center Science and Technology Project "Breeding and Evaluation of Drought-resistant Iris Excellent Varieties" (ZX2019010).

Data Availability Statement: Data is available in the Supplementary Materials.

Conflicts of Interest: The authors declare no conflicts of interest.

References

1. Liu, L.L.; Cao, X.D.; Xu, Z.R.; Zhang, J.F.; Wu, Y.H. Studies on Floral Syndrome and Mating System of Iris halophila. *Acta Agrestia Sinica* **2021**, *29*, 2731–2741.
2. Knudsen, J.T.; Eriksson, R.; Gershenzon, J.; Stahl, B. Diversity and distribution of floral scent. *Bot. Rev.* **2006**, *72*, 1. [CrossRef]
3. Patel, S.; Shibamoto, T. Flavor compounds in wines produced from Chardonnay grapes fermented with fruit juices. *Food Sci. Technol. Res.* **2003**, *9*, 84–86. [CrossRef]
4. Pichersky, E.; Raguso, R.A.; Lewinsohn, E.; Croteau, R. Floral scent production in Clarkia (Onagraceae) (I. Localization and developmental modulation of monoterpene emission and linalool synthase activity). *Plant Physiol.* **1994**, *106*, 1533–1540. [CrossRef] [PubMed]
5. Yuan, Y.; Sun, Y.; Zhao, Y.; Liu, C.; Chen, X.; Li, F.; Bao, J. Identification of Floral Scent Profiles in Bearded Irises. *Molecules* **2019**, *24*, 1773. [CrossRef] [PubMed]
6. Shalit, M.; Guterman, I.; Volpin, H.; Bar, E.; Tamari, T.; Menda, N.; Adam, Z.; Zamir, D.; Vainstein, A.; Weiss, D.; et al. Volatile ester formation in roses Identification of an acetyl-coenzyme A. Geraniol/Citronellol acetyltransferase in developing rose petals. *Plant Physiol.* **2003**, *131*, 1868–1876. [CrossRef] [PubMed]
7. D'Auria, J.C.; Chen, F.; Pichersky, E. Characterization of an acyltransferase capable of synthesizing benzyl-benzoate and other volatile esters in flowers and damaged leaves of *Clarkia breweri*. *Plant Physiol.* **2002**, *130*, 466–476. [CrossRef]
8. Zhang, W.; He, C.; Gong, Y. Pollinator attraction and outcrossing strategies in Iris. *Plant Sci. J.* **2019**, *37*, 672–681.
9. Li, C.; Gao, Y.; Liu, R.; Cao, Y.; Fan, Z.; Guo, L.; Zhang, Q. Analysis on the barriers of interspecific hybridization in beardless Irises. *J. Beijing For. Univ.* **2018**, *40*, 96–101.
10. Qi, J.; Zhai, Y.; Zhao, C. The Chemical Constituents of Genus Irisand Their Biological Activitie. *Nat. Prod. Res. Dev.* **2006**, *18*, 165–170.
11. Wang, W.; Wang, P.; Qiao, Q.M. Research on the Classification and Application Value of Iris Plant. *J. Anhui Agric. Sci.* **2008**, *36*, 1001–1002. (In Chinese)
12. Cai, K.; Feng, C.; Xu, S.; Sun, Y.; Lou, Q.; Sun, J.; Chen, H. The volatile components in different flowering stages of *Iris uniflora*. *J. Northeast. For. Univ.* **2023**, *51*, 53–58.
13. Cai, K.; Tian, K.; Ban, Z.; Xu, H.; Jia, W.; Zhu, Y.; Chen, H. Analysis of Floral Fragrance Components in Different Parts of *Iris typhifolia*. *Horticulturae* **2023**, *9*, 1268. [CrossRef]
14. Başer, K.H.; Demirci, B.; Orhan, I.E.; Kartal, M.; Sekeroglu, N.; Sener, B. Composition of Volatiles from Three Iris Species of Turkey. *J. Essent. Oil Res.* **2018**, *23*, 66–71. [CrossRef]
15. Zito, P.; Rosselli, S.; Bruno, M.; Maggio, A.; Sajeva, M. Floral scent in Iris planifolia (Iridaceae) suggests food reward. *Phytochemistry* **2019**, *158*, 76–90. [CrossRef]
16. Jia, X.; Deng, Q.; Yang, Y.; Xiang, X.; Zhou, X.; Tan, C.; Zhou, Q.; Huang, F. Unraveling of the Aroma-Active Compounds in Virgin Camellia Oil (*Camellia oleifera* Abel) Using Gas Chromatography–Mass Spectrometry–Olfactometry, Aroma Recombination, and Omission Studies. *J. Agric. Food Chem.* **2021**, *69*, 9043–9055. [CrossRef]
17. Zhang, T.; Bao, F.; Yang, Y.; Hu, L.; Ding, A.; Ding, A.; Ding, A.; Wang, J.; Cheng, T.; Zhang, Q. A Comparative Analysis of Floral Scent Compounds in Intraspecific Cultivars of *Prunus mume* with Different Corolla Colours. *Molecules* **2020**, *25*, 145. [CrossRef]
18. Lu, X.L.; Hai, Z.; Wang, J. Detection of Cola beverage by electronic nose. *J. Zhejiang Univ. Agric. Life Sci.* **2006**, *32*, 677–682.
19. Liu, X.; Wang, W.; Fang, S. Thermodynamic studies on NO radical with 2,3-dimethylpentantal. *Petrochem. Ind. Appl.* **2011**, *30*, 4.
20. SJaeger, R.; Pineau, B.; Bava, C.M.; Atkinson, K.R.; McRae, J.F.; Axten, L.G.; Chheang, S.L.; Beresford, M.K.; Peng, M.; Paisley, A.G.; et al. Investigation of the impact of sensitivity to cis-3-hexenol (green/grassy) on food acceptability and selection. *Food Qual. Prefer.* **2012**, *24*, 230–242. [CrossRef]
21. León, D.C.S.; Ortíz, D.K.R.; González, D.F.J. Sensory approach and chiral analysis for determination of odour active compounds from feijoa (*Acca sellowiana*). *Food Chem.* **2020**, *317*, 126383. [CrossRef]
22. Jin, K.S.; Bak, M.J.; Jun, M.; Lim, H.J.; Jo, W.K.; Jeong, W.S. α-Pinene Triggers Oxidative Stress and Related Signaling Pathways in A549 and HepG2 Cells. *Food Sci. Biotechnol.* **2010**, *19*, 1325–1332. [CrossRef]
23. Hyun, J.; Lee, J.G.; Yang, K.Y.; Lim, S.; Lee, E.J. Postharvest Fumigation of (E)-2-Hexenal on Kiwifruit (*Actinidia chinensis* cv. 'Haegeum') Enhances Resistance to Botrytis cinerea. *Postharvest Biol. Technol.* **2022**, *187*, 111854. [CrossRef]

24. Garcia, L.; Perrin, C.; Nolleau, V.; Godet, T.; Farines, V.; Garcia, F.; Caillé, S.; Saucier, C. Impact of Acetaldehyde Addition on the Sensory Perception of Syrah Red Wines. *Foods* **2022**, *11*, 1693. [CrossRef] [PubMed]
25. Han, Y.; Shen, H.; Zhao, M.; Sun, W. Flavour binding mechanism between a typical meat flavour compound (nonanal) and porcine myofibrillar proteins with consideration of conformational changes. *Int. J. Food Sci. Technol.* **2018**, *53*, 1954–1961. [CrossRef]
26. Iyer, M.M.; Sacks, G.L.; Padilla-Zakour, O.I. Impact of Harvesting and Processing Conditions on Green Leaf Volatile Development and Phenolics in Concord Grape Juice. *J. Food Sci.* **2010**, *75*, C297–C304. [CrossRef] [PubMed]
27. Kaneda, N.; Lee, I.S.; Gupta, M.P.; Soejarto, D.D.; Kinghorn, A.D. (+)-4β-Hydroxyhernandulcin, A New Sweet Sesquiterpene from the Leaves and Flowers of Lippia dulcis. *J. Nat. Prod.* **1992**, *55*, 1136–1141. [CrossRef]
28. Neelam Singh-Sangwan, N.S.S.; Sangwan, R.S.; Rajesh Luthra, R.L.; Thakur, R.S. Geraniol Dehydrogenase: A Determinant of Essential Oil Quality in Lemongrass. *Planta Medica* **1993**, *59*, 168–170. [CrossRef] [PubMed]
29. Mostafavi, A.; Shamspur, T.; Afazali, D. Chemical Composition of the Essential Oil of *Ducrosia assadii* Alava. from Kerman Province in Iran. *J. Essent. Oil Res.* **2010**, *22*, 300–302. [CrossRef]
30. Van Aardt, M.; Duncan, S.E.; Marcy, J.E.; Long, T.E.; Nielsen-Sims, S.R. Aroma Analysis of Light-Exposed Milk Stored with and Without Natural and Synthetic Antioxidants. *J. Dairy Sci.* **2005**, *88*, 881–890. [CrossRef] [PubMed]
31. Xia, H.; Gao, H.; Sun, Q.; Wu, F.; Ge, T.; Sui, K.; Wang, Z.; Song, L.; Huang, X.; Yu, Q. Puerarin, an efficient natural stabilizer for both polyethylene and polypropylene. *J. Appl. Polym. Sci.* **2020**, *137*, e49599. [CrossRef]
32. Satoh, M.; Kusumoto, N.; Matsui, N.; Makino, R.; Hashida, K.; Arai, D.; Iiduka, Y.; Ashitani, T. Antitermitic and antifungal properties of enantiopure linalool and furanoid linalool oxide confirmed in *Lindera umbellata* var. *membranacea*. *J. Wood Chem. Technol.* **2021**, *42*, 37–45. [CrossRef]
33. Castellar, A.; Oliveira, D.R.; Leitão, S.G.; Bizzo, H.R.; Soares MD, L.C.; Kinupp, V.F.; Veiga-Junior, V.F. Essential oil from Philodendron fragrantissimum, an aromatic Araceae from Amazonia, Brazil. *J. Essent. Oil Res.* **2013**, *25*, 194–197. [CrossRef]
34. Wolken, W.A.M.; Tramper, J.; van der Werf, M.J. Amino acid-catalyzed retroaldol condensation: The production of natural benzaldehyde and other flavour compounds. *Flavour Fragr. J.* **2004**, *19*, 115–120. [CrossRef]
35. Dong, Y.; Li, X.; Zhao, Y.; Ren, X.; Zheng, Y.; Song, R.; Zhong, X.; Shan, D.; Lv, F.; Deng, Q.; et al. Biotransformation and metabolism of three methyl salicylate glycosides by gut microbiota in vitro. *J. Pharm. Biomed. Anal.* **2023**, *233*, 115474. [CrossRef] [PubMed]
36. Kato, Y.; Yuasa, Y. Practical Synthesis of 3-Methylnonane-2,4-dione, an Intense Strawlike and Fruity Flavored Compound. *J. Agric. Food Chem.* **2001**, *49*, 3864–3866. [CrossRef] [PubMed]
37. Kim, H.J.; Chen, F.; Wu, C.; Wang, X.; Chung, H.Y.; Jin, Z. Evaluation of Antioxidant Activity of Australian Tea Tree (*Melaleuca alternifolia*) Oil and Its Components. *J. Agric. Food Chem.* **2004**, *52*, 2849–2854. [CrossRef] [PubMed]
38. Hou, H.; Zhang, X.; Zhao, T.; Zhou, L. Effects of Origanum vulgare essential oil and its two main components, carvacrol and thymol, on the plant pathogen Botrytis cinerea. *PeerJ* **2020**, *8*, e9626. [CrossRef] [PubMed]
39. Kim, M.G.; Lee, H.S. Growth-inhibiting Effects and Chemical Composition of Essential Oils Extracted from *Platycladus orientalis* Leaves and Stemstoward Human Intestinal Bacteria. *Food Sci. Biotechnol.* **2015**, *24*, 427–431. [CrossRef]
40. Raice, R.T.; Sjoholm, I.; Wang, H.L.; Bergenståhl, B. Characterization of volatile components extracted from *Vangueria infausta* (African medlar) by using GC–MS. *J. Essent. Oil Res.* **2015**, *27*, 76–81. [CrossRef]
41. Sun, J.; Chin, J.H.; Zhou, W.; Yu, B.; Curran, P.; Liu, S.Q. Biocatalytic Conversion of Coconut Oil to Natural Flavor Esters Optimized with Response Surface Methodology. *J. Am. Oil Chem. Soc.* **2012**, *89*, 1991–1998. [CrossRef]
42. Wang, L.; Dou, G.; Guo, H.; Zhang, Q.; Qin, X.; Yu, W.; Xiao, H. Volatile organic compounds of *Hanseniaspora uvarum* increase strawberry fruit flavor and defense during cold storage. *Food Sci. Nutr.* **2019**, *7*, 2625–2635. [CrossRef] [PubMed]
43. Kafkas, E.; Cabaroglu, T.; Selli, S.; Bozdoğan, A.; Kürkçüoğlu, M.; Paydaş, S.; Başer, K.H.C. Identification of volatile aroma compounds of strawberry wine using solid-phase microextraction techniques coupled with gas chromatography–mass spectrometry. *Flavour Fragr. J.* **2006**, *21*, 68–71. [CrossRef]
44. Plesage, L.; Candy, J.P.; Hirigoyen, C.; Humblot, F.; Basset, J.M. Selective dehydrogenation of dipentene (R-(+)-limonene) into paracymene on silica supported palladium assisted by α-olefins as hydrogen acceptor. *J. Mol. Catal. A Chem.* **1996**, *112*, 431–435. [CrossRef]
45. Procida, G.; Lagazio, C.; Cateni, F.; Zacchigna, M.; Cichelli, A. Characterization of arabica and robusta volatile coffees composition by reverse carrier gas headspace gas chromatography–mass spectrometry based on a statistical approach. *Food Sci. Biotechnol.* **2020**, *29*, 1319–1330. [CrossRef]
46. Effimia, E.; Karabagias, I.K.; Sofia, M.; Dionysios, K.; Nikolaos, K. Geographical origin discrimination of "Ntopia" olive oil cultivar from ionian islands using volatile compounds analysis and computational statistics. *Eur. Food Res. Technol. Z. Lebensm. Unters. Forschung. A* **2021**, *247*, 3083–3098.
47. Gupta, S.; Gaurav, B.; Dwivedi, D.G.; Srivastava, K. Antimycobacterial activity of fractions and isolated compounds from *Vetiveria zizanioides*. *Med. Chem. Res.* **2012**, *21*, 1283–1289. [CrossRef]

Disclaimer/Publisher's Note: The statements, opinions and data contained in all publications are solely those of the individual author(s) and contributor(s) and not of MDPI and/or the editor(s). MDPI and/or the editor(s) disclaim responsibility for any injury to people or property resulting from any ideas, methods, instructions or products referred to in the content.